Research Square

Preprints are preliminary reports that have not undergone peer review.
They should not be considered conclusive, used to inform clinical practice,
or referenced by the media as validated information.

NR1D1 Suppresses Retinoblastoma Growth via the ROS/AKT/mTOR Axis: Therapeutic Implications of REV-ERBα Agonism

Yinan Han

yinanhan20210126.com

Eye & ENT Hospital of Fudan University https://orcid.org/0000-0001-6137-694X

Jinghan Wang

Eye & ENT Hospital of Fudan University

Jie Ding

Eye & ENT Hospital of Fudan University

Lu Gan

Eye & ENT Hospital of Fudan University

Rui Huang

Eye & ENT Hospital of Fudan University

Jiang Qian

Eye, Ear, Nose, and Throat Hospital of Fudan University

Article

Keywords:

Posted Date: November 20th, 2026

DOI: https://doi.org/10.21203/rs.3.rs-11409783/v1

License: This work is licensed under a Creative Commons Attribution 4.0 International License.
Read Full License

Additional Declarations: (Not answered)

NR1D1 Suppresses Retinoblastoma Growth via the ROS/AKT/mTOR Axis: Therapeutic Implications of *REV-ERB α* Agonism

Jinghan Wang[#], Jie Ding[#], Lu Gan, Rui Huang, Jiang Qian, Yinan Han*
Department of Ophthalmology, Eye & ENT Hospital of Fudan University, 83 Fenyang Road, Xuhui District, Shanghai 200031, China e-mail: wangjinghan68@126.com
*Corresponding authors. Email: yinanhan2021@126.com

The authors declare that they have no known competing financial interests or personal relationships that could have appeared to influence the work reported in this paper.

Abstract

Purpose: To investigate clock gene expression in retinoblastoma (RB) and explore the role and mechanism of nuclear receptor subfamily 1 group D member 1 (*NR1D1*) in RB progression.
Methods: Bioinformatics analysis of the GSE58780 dataset was used to identify differentially expressed genes and clock genes in RB. The level of *NR1D1* in RB tissues and cells was determined by qPCR, Western blot, and immunohistochemistry. Its role in RB was explored through gain-of-function and loss-of-function experiments. Cell growth, migration, invasion, and apoptosis were evaluated by CCK-8, EdU, Transwell, and flow cytometry. ROS levels and AKT/mTOR pathway activation were measured by flow cytometry and Western blot. A xenograft model of RB was established to explore the role of SR9009 in vivo.
Results: In RB samples, clock genes *CRY1*, *NR1D1*, *NR2E3*, and *TOX* were significantly downregulated, while *TIMELESS* was upregulated. *NR1D1* was confirmed to be significantly reduced in RB tissues. *NR1D1* knockdown enhanced RB cell proliferation, migration, and invasion and inhibited apoptosis. In addition, ROS levels and the AKT/mTOR pathway was inhibited by *NR1D1*. In vivo, *NR1D1* agonist SR9009 markedly restrained tumor growth, promoted apoptosis, and reduced AKT and mTOR phosphorylation.
Conclusion: Clock genes are abnormally expressed in RB, with *NR1D1* significantly downregulated. *NR1D1* regulates RB growth through the ROS/AKT/mTOR pathway, and its agonist SR9009 inhibits RB tumor growth by activating *NR1D1*. These findings provide a potential therapeutic target for RB treatment.

Introduction

Retinoblastoma (RB) is the most common primary intraocular malignancy in children, and survival remains dependent on early diagnosis and effective intervention[1]. Although current treatments, including chemotherapy and enucleation, have improved outcomes, they are associated with severe long-term complications and remain inadequate for advanced or metastatic disease [2-3]. These challenges highlight the urgent need to identify novel molecular drivers and therapeutic targets beyond canonical *RB1* inactivation, which cannot fully explain tumor invasion, progression, or heterogeneity [2].

In recent years, circadian clock disruption has emerged as a key hallmark of cancer. The circadian clock system, governed by a core network of transcriptional–translational feedback loops, regulates cell cycle progression, metabolism, DNA repair, apoptosis, and redox balance [4]. Orphan nuclear receptors, including *NR1D1* (*REV-ERBα*) and *NR2E3*, are critical components of the circadian clock and play essential roles in retinal development and tumor suppression [5]. Accumulating evidence indicates that *NR1D1* acts as a tumor suppressor in multiple cancers, including bladder cancer, lung cancer, and ovarian cancer [6-8]. Similarly, *NR2E3* is essential for retinal photoreceptor differentiation and has been implicated in suppressing breast and liver cancer [9-10].

Our previous clinical study of 51 retinoblastoma specimens demonstrated that *NR1D1* and *NR2E3* were significantly downregulated in RB tissues compared with normal retina[11]. Importantly, low expression of *NR1D1* was significantly associated with advanced IIRC stage, choroidal invasion, and optic nerve invasion, while low *NR2E3* expression correlated with high-risk pathology, tumor necrosis, and aggressive clinicopathological features [11]. These findings strongly suggest that *NR1D1* and *NR2E3* may function as tumor suppressors in RB. However, the functional role and underlying mechanism of *NR1D1* in RB proliferation, invasion, and survival remain largely unknown.

In this study, we focused on *NR1D1* to systematically investigate its biological function and molecular mechanism in retinoblastoma. We hypothesized that *NR1D1* suppresses RB progression by regulating intracellular reactive oxygen species (ROS) and the AKT/mTOR signaling pathway. We validated *NR1D1* downregulation in clinical RB samples and performed gain- and loss- of- function assays in vitro. We further explored the NR1D1–ROS–AKT/mTOR axis and confirmed the therapeutic potential of the *NR1D1* agonist SR9009 in a xenograft model. This study bridges circadian biology and pediatric oncology, establishing *NR1D1* as a novel tumor suppressor and promising therapeutic target in retinoblastoma.

Materials and Methods

Retinoblastoma (RB) Tissues and Normal Retinal Tissue Collection

Fifty-one paraffin-embedded retinoblastoma (RB) specimens and 12 normal retinal tissues were collected at the Eye & ENT Hospital of Fudan University between 2018 and 2023. Normal retinal tissues were obtained from patients undergoing orbital exenteration for eyelid or orbital malignancies that did not involve the globe. All RB patients underwent primary enucleation without prior anticancer therapy. Freshly resected tumor specimens were immediately placed in pre-chilled cryotubes, snap-frozen in liquid nitrogen, and stored at −80°C for subsequent nucleic acid and protein extraction. For immunohistochemistry, RB tissues were fixed immediately in eyeball-specific fixative and processed for paraffin embedding and sectioning using standard protocols. Written informed consent was obtained from all participants or their legal guardians. This study was approved by the Institutional Review Board and Ethics Committee of the Eye & ENT Hospital of Fudan University.

Bioinformatics Analysis

The GSE58780 gene expression dataset was retrieved from the NCBI Gene Expression Omnibus (GEO) database using the GEOquery R package. Raw microarray data were normalized using the Robust Multi-array Average (RMA) algorithm. Data quality was verified by principal component analysis (PCA) and sample clustering. Three RB samples (GSM5121298, GSM5121309, GSM5121313) and three normal retinal samples (GSM5121346, GSM5121347, GSM5121348) were selected for differential expression analysis. The limma R package was used to identify differentially expressed genes (DEGs). Genes with $|\log2(\text{fold change})| > 1$ and adjusted $*P* < 0.05$ were defined as significant DEGs. Volcano plots were generated using the ggplot2 R package for visualization.

Transcriptomic Analyses

Total RNA was isolated from three normal retinal tissues and three RB tissues using the Tissue RNA Purification Kit (EZBioscience). RNA purity and concentration were determined using a NanoDrop 2000 spectrophotometer (Thermo Fisher Scientific). Extracted RNA was reverse-transcribed into cDNA using the PrimeScript™ RT Master Mix Kit (TaKaRa Bio). Quantitative real-time PCR (qRT-PCR) was performed according to the manufacturer's instructions.

Cell Transfection

Cells were seeded in 12-well plates at a density of 1×10^5 cells per well. Lentiviruses carrying *NR1D1* short hairpin RNA (shRNA) or control shRNA were added at a multiplicity of infection (MOI) of 2 for Weri-Rb1 cells and 20 for Y79 cells, in the presence of 4 μg/mL Polybrene. Plates were sealed with Parafilm and centrifuged at 200 × *g* for 60 minutes at room temperature to enhance infection efficiency. The shRNA sequences targeting *NR1D1* were:

- sh*NR1D1*-1: 5′-GGAGTCTACAAGTGGCCAT-3′
- sh*NR1D1*-2: 5′-GCTGAATGGCATGGTGTTA-3′

Quantitative Real-Time PCR (qRT-PCR)

Total RNA was extracted using a high-purity RNA isolation kit (TaKaRa Bio). qRT-PCR was performed to quantify mRNA expression of *NR1D1*, with GAPDH as an internal control. Primer sequences were as follows:
- *NR1D1* forward: 5′-TGGACTCCAACAACAACACAG-3′
- *NR1D1* reverse: 5′-GATGGTGGGAAGTAGGTGGG-3′
- GAPDH forward: 5′-GGAGCGAGATCCCTCCAAAAT-3′
- GAPDH reverse: 5′-GGCTGTTGTCATACTTCTCATGG-3′

Western Blotting
Total protein was extracted from cells or tissues using RIPA lysis buffer supplemented with protease and phosphatase inhibitors. Protein concentration was measured using a BCA protein assay kit (Beyotime). Equal amounts of protein were separated by 10–12% SDS-PAGE and transferred to PVDF membranes. Membranes were blocked in 5% non-fat milk in TBST for 1 hour at room temperature, then incubated with primary antibodies against *NR1D1* (1:1000; Proteintech) and GAPDH (1:1000; Cell Signaling Technology) overnight at 4°C. After washing in TBST, membranes were incubated with HRP-conjugated secondary antibodies (1:10,000; Proteintech) for 1 hour at room temperature. Protein bands were visualized using ECL reagent and imaged using a ChemiDoc imaging system (Bio-Rad).

Cell Viability and Proliferation Assays
Cell viability was assessed using Cell Counting Kit-8 (CCK-8; Dojindo). Logarithmically growing cells were seeded in 96-well plates at 1×10^4 cells per well. At 0, 6, 24, 48, and 72 hours, 10 μL CCK-8 solution was added to each well and incubated for 1 hour. Absorbance at 450 nm was measured using a BioTek microplate reader.
For proliferation assays, 1×10^6 cells were seeded in 6-well plates and cultured for 2 hours. The medium was replaced with fresh medium containing 10 μM EdU (Beyotime) and incubated for 2 hours. After permeabilization with 0.5% Triton X-100 and blocking with 3% BSA, cells were processed using the EdU staining kit according to the manufacturer's protocol and imaged under a fluorescence microscope.

Flow Cytometry
Cell apoptosis was evaluated using an Annexin V-PE/7-AAD apoptosis detection kit (Sungenebiotech). Cells were stained and incubated in the dark for 5 minutes before flow cytometric analysis.
For intracellular reactive oxygen species (ROS) measurement, cells were incubated with 100 μL DHE staining working solution (Yeasen) at 37°C for 60 minutes and analyzed by flow cytometry.

Transwell Invasion Assay
Matrigel (Corning) was diluted 1:9 in cold serum-free medium. A 50 μL aliquot was added to the upper chamber of Transwell inserts and incubated at 37°C for 1 hour to allow gelation. A total of 5×10^4 cells suspended in serum-free medium were seeded

into the upper chamber, and complete medium containing FBS was added to the lower chamber. After 24 hours of incubation, invaded cells were fixed in 4% paraformaldehyde for 20 minutes, stained with crystal violet, and counted under a microscope.

Animal Studies

Four-week-old male BALB/c nude (nu/nu) mice were purchased from Jihui Bioscience. Mice were subcutaneously injected in the right axillary fossa with 100 μL Weri-Rb1 cell suspension. After 7 days, mice were randomly assigned to receive daily intraperitoneal injections of SR9009 (100 mg/kg) or vehicle (normal saline containing 10% DMSO) for 3 consecutive weeks. SR9009 was dissolved in 10% DMSO in normal saline at a concentration of 10 mg/mL. At the end of treatment, mice were euthanized, and tumors were dissected, weighed, and processed for histologic and immunohistochemical analyses. All animal experiments were performed in accordance with institutional guidelines for laboratory animal care and use.

Hematoxylin and Eosin (H&E) Staining

Harvested tumor tissues were fixed, paraffin-embedded, and sectioned at 4 μm. After deparaffinization and rehydration, sections were stained with standard H&E for histologic examination.

Immunohistochemistry (IHC)

Paraffin sections were deparaffinized, rehydrated, and subjected to antigen retrieval in citrate buffer. Endogenous peroxidase activity was blocked with 3% H_2O_2 for 10 minutes, followed by blocking in 5% BSA for 30 minutes. Sections were incubated with primary antibodies overnight at 4°C, then with HRP-conjugated secondary antibodies for 1 hour at room temperature. Staining was developed using DAB chromogen, counterstained with hematoxylin, dehydrated, cleared, and mounted for microscopic evaluation.

TUNEL Assay

Paraffin sections were deparaffinized, rehydrated, and permeabilized with 0.1% Triton X-100 in PBS for 20 minutes at room temperature. TUNEL staining was performed using a TUNEL apoptosis detection kit (Ruchuang Bio) according to the manufacturer's instructions. Nuclei were counterstained with DAPI. Images were acquired using a fluorescence microscope.

Statistical Analysis

Data were analyzed and visualized using GraphPad Prism 8.0.2 software. Quantitative data are presented as mean ± standard deviation (SD), and qualitative data as frequency (percentage). Normality was assessed using the Shapiro–Wilk test. Normally distributed data were compared using two-tailed independent samples t-test; non-normally distributed data were analyzed using the Wilcoxon rank-sum test. One-

way ANOVA was used for comparisons among three or more groups. A P value < 0.05 was considered statistically significant.

Results

Clock Genes Are Dysregulated in Retinoblastoma in the GSE58780 Dataset

We analyzed the GSE58780 gene expression dataset from the GEO database to identify differentially expressed genes (DEGs) in retinoblastoma (RB). A total of 2363 DEGs were identified, comprising 1156 downregulated and 1207 upregulated genes in RB relative to normal retina (Fig. 1A). We next focused on 15 core clock genes: *CLOCK*, *PER1*, *PER2*, *PER3*, *CRY1*, *CRY2*, *NR1D1*, *NR1D2*, *NR2E3*, *RORA*, *RORC*, *AANAT*, *TOX*, *TIMELESS*, and *CSNK1D* (Fig. 1B). Compared with normal retinal tissues, RB tissues exhibited significantly reduced expression of *CRY1* (P < 0.01), *NR1D1* (P < 0.01), *NR2E3* (P < 0.001), and *TOX* (P < 0.001), whereas *TIMELESS* expression was markedly increased (P < 0.001). These data indicate that dysregulation of clock genes is a common feature of RB and may contribute to tumorigenesis.

NR1D1 Expression Is Markedly Downregulated in Human RB Tissues

We validated the expression of the 15 clock genes in 3 normal retinal tissues and 3 RB tissues using qRT-PCR. Among these genes, *NR1D1* was significantly downregulated at the mRNA level in RB tissues (Fig. 1C). Western blotting confirmed that NR1D1 protein expression was also drastically reduced in RB (P < 0.001; Fig. 1D). Collectively, these findings demonstrate that *NR1D1* is consistently downregulated in RB, suggesting a potential tumor-suppressive role.

Knockdown of *NR1D1* Enhances Proliferation, Migration, Invasion, and Suppresses Apoptosis in RB Cells

To investigate the function of *NR1D1* in RB, we knocked down *NR1D1* in Weri-Rb1 and Y79 cells using two independent shRNAs(Fig. 2A). Both shRNAs significantly reduced *NR1D1* mRNA and protein levels (Fig. 2B); sh*NR1D1*-2 was used for subsequent assays. CCK-8 assays revealed that *NR1D1* silencing markedly accelerated the proliferation of Weri-Rb1 and Y79 cells (Fig. 2C). EdU incorporation assays confirmed a higher proportion of proliferating cells following *NR1D1* knockdown (Fig. 2D). Transwell assays showed that migration and invasion capacities were significantly increased in *NR1D1*-deficient RB cells (Fig. 2E). Western blotting demonstrated that *NR1D1* knockdown decreased Bax expression, increased Bcl-2 expression, and reduced the Bax/Bcl-2 ratio (Fig. 2F). Flow cytometry further confirmed that silencing *NR1D1* significantly inhibited RB cell apoptosis (Fig. 2G).

Overexpression of *NR1D1* Restricts Proliferation, Migration, Invasion, and Induces Apoptosis in RB Cells

We next overexpressed *NR1D1* in Weri-Rb1 and Y79 cells; qRT-PCR and Western blotting verified successful overexpression (Figs. 3A and B). CCK-8 assays showed that *NR1D1* overexpression significantly suppressed the viability of RB cells (Fig. 3C). EdU assays revealed a lower percentage of proliferating cells in the *NR1D1*-overexpressing group (Fig. 3D). Transwell assays demonstrated that ectopic *NR1D1* expression markedly attenuated migration and invasion (Fig. 3E). Western blotting showed increased Bax, decreased Bcl-2, and an elevated Bax/Bcl-2 ratio upon *NR1D1* overexpression (Fig. 3F). Flow cytometry confirmed that enforced *NR1D1* expression significantly induced apoptosis in RB cells (Fig. 3G).

NR1D1 Modulates ROS Levels and the AKT/mTOR Signaling Pathway in RB Cells

We next examined the relationship between *NR1D1*, oxidative stress, and AKT/mTOR signaling. *NR1D1* knockdown significantly increased intracellular ROS levels, whereas *NR1D1* overexpression reduced ROS production (Fig. 4A). Western blotting revealed that silencing *NR1D1* enhanced the phosphorylation of AKT and mTOR, indicating pathway activation; conversely, *NR1D1* overexpression inhibited AKT/mTOR signaling (Figs. 4B and C). To establish a causal link, we treated RB cells with the ROS inducer rotenone and the ROS scavenger N-acetylcysteine (NAC). Elevated ROS activated the AKT/mTOR pathway, whereas ROS inhibition suppressed AKT/mTOR activity (Fig. 4D). These results indicate that *NR1D1* negatively regulates AKT/mTOR signaling by modulating intracellular ROS levels.

Rapamycin Reverses the Oncogenic Effects Induced by *NR1D1* Knockdown in RB Cells

We treated RB cells with the mTOR inhibitor rapamycin (Rapa), which dose-dependently suppressed AKT/mTOR signaling (Fig. 5A). We then established four experimental groups: (1) shControl, (2) sh*NR1D1*, (3) shControl + Rapa, and (4) sh*NR1D1* + Rapa. CCK-8 and EdU assays showed that rapamycin rescued the enhanced proliferation caused by *NR1D1* knockdown (Figs. 5B and C). Transwell assays demonstrated that rapamycin also reversed the enhanced migration and invasion induced by *NR1D1* silencing (Fig. 5D). These data confirm that the effects of *NR1D1* on RB progression are mediated, at least in part, through the AKT/mTOR pathway.

The *NR1D1* Agonist SR9009 Inhibits RB Growth in Xenograft Mouse Models

To assess the therapeutic potential of *NR1D1* activation, we established a subcutaneous RB xenograft model and treated mice with the *NR1D1* agonist SR9009.

SR9009 treatment significantly reduced tumor volume and weight (Fig. 6A). IHC staining showed lower Ki-67 positivity in SR9009-treated tumors, indicating reduced proliferation (Fig. 6B). TUNEL assays revealed a higher proportion of apoptotic cells in the SR9009 group (Fig. 6C). Finally, Western blotting of tumor tissues showed that SR9009 increased *NR1D1* expression and decreased p-AKT and p-mTOR levels, confirming inhibition of the AKT/mTOR pathway in vivo (Fig. 6D).

Discussion

Retinoblastoma is the most common pediatric intraocular malignancy, and advanced tumors with choroidal or optic nerve invasion continue to pose significant therapeutic challenges [1]. Beyond classical RB1 inactivation, the molecular mechanisms driving RB invasion and progression remain poorly understood [12]. Circadian clock dysregulation has emerged as a critical factor in tumorigenesis; however, its role in RB has not been systematically defined [13]. Our previous work in 51 clinical RB specimens demonstrated that *NR1D1* and *NR2E3* were significantly downregulated in RB tissues, and their low expression was closely associated with advanced stage, choroidal invasion, optic nerve invasion, and high-risk pathology [11]. These clinical findings provided the rationale for the present mechanistic study.

In this study, we confirmed that *NR1D1* is consistently downregulated in human RB tissues at both mRNA and protein levels. Functional experiments demonstrated that *NR1D1* acts as a tumor suppressor by inhibiting proliferation, migration, invasion, and promoting apoptosis in RB cells. Mechanistically, we identified a novel NR1D1–ROS–AKT/mTOR signaling axis that regulates RB progression. Downregulation of *NR1D1* increased intracellular ROS levels, which in turn activated the AKT/mTOR pathway, promoting malignant phenotypes. Pharmacological inhibition of mTOR by rapamycin reversed the oncogenic effects induced by *NR1D1* knockdown, confirming the causal relationship in this pathway [14]. These findings extend our earlier clinical observations by defining the molecular mechanism through which *NR1D1* loss promotes RB aggressiveness. An important open question is how *NR1D1* governs intracellular ROS homeostasis in retinoblastoma. In retinal pigment epithelium, *NR1D1* directly regulates transcription of the master antioxidant transcription factor NRF2 and its downstream effectors SOD1 and catalase, and pharmacological activation of *NR1D1* protects RPE cells from oxidative damage in vivo and in vitro [19]. Given that *NR1D1* acts as a transcriptional repressor of core clock genes and controls redox-related transcriptional programs, we speculate that *NR1D1* may restrain ROS accumulation in retinoblastoma at least partly through transcriptional regulation of antioxidant gene programs, a hypothesis that could be tested by chromatin immunoprecipitation and antioxidant-response element reporter assays in future studies. Elucidating these upstream regulatory mechanisms would further anchor the NR1D1–ROS axis within the broader circadian–redox network and may uncover additional druggable nodes beyond SR9009.

Our results are consistent with the tumor-suppressive role of *NR1D1* reported in other cancers [6-7]. *NR1D1* has been shown to inhibit proliferation and metastasis in bladder cancer, lung cancer, and hepatocellular carcinoma by regulating multiple oncogenic signaling pathways [6,8,15]. Our study provides the first mechanistic evidence that *NR1D1* suppresses retinoblastoma through redox regulation and AKT/mTOR signaling. Notably, our previous clinical data showed that low *NR1D1* expression was associated with choroidal and optic nerve invasion [11]; the present study further demonstrates that *NR1D1* directly inhibits migration and invasion, providing a biological explanation for these clinical correlations.

Although our previous study focused on both *NR1D1* and *NR2E3* [11], the present study prioritized *NR1D1* because of its well-established role as a circadian nuclear receptor and its robust downregulation in bioinformatic analyses. *NR2E3* is primarily involved in retinal photoreceptor differentiation [16], and its mechanism in RB warrants separate investigation. Nevertheless, our collective findings support that orphan nuclear receptors of the circadian clock represent a novel class of tumor suppressors in retinoblastoma.

The NR1D1–ROS–AKT/mTOR axis identified in this study also has implications for the tumor microenvironment. Loss of *NR1D1* leads to ROS accumulation, which promotes inflammation and immune suppression [17]. Hyperactivated AKT/mTOR signaling further reshapes immune cell infiltration and function [18]. *NR1D1* agonists such as SR9009 may therefore exert dual antitumor effects: direct suppression of tumor cell malignancy and indirect remodeling of the immune microenvironment. This provides a rationale for combining *NR1D1*-targeted therapy with chemotherapy or immunotherapy for advanced RB.

Beyond its direct tumor-suppressive effects, activation of *NR1D1* may sensitize retinoblastoma to established therapeutic modalities, a possibility with direct clinical relevance [19-21]. In multiple myeloma, the *REV-ERBα* agonist SR9009 suppresses GRP78-dependent autophagy and *de novo* lipogenesis and exerts synergistic cytotoxicity with the proteasome inhibitor bortezomib in both cell lines and xenograft models, suggesting that *REV-ERBα* agonism can augment conventional chemotherapy [20]. In breast cancer, *NR1D1* activates cGAS–STING signaling, enhances type I interferon-mediated antitumor immunity, and its pharmacological activation by SR9009 suppresses tumor progression and lung metastasis [21]. Given that the AKT–mTOR pathway controls PD-L1 expression in several tumor types [18], the NR1D1–ROS–AKT/mTOR axis delineated here may also shape immune checkpoint expression in retinoblastoma, providing a rationale for combining *NR1D1*-targeted therapy with immunotherapy. Notably, because the clinical activity of immune checkpoint blockade depends on an inflamed tumor microenvironment, strategies that simultaneously reduce tumor-cell-intrinsic ROS burden and remodel immune

infiltration—such as *REV-ERBα* agonism—warrant evaluation in orthotopic and immune-competent retinoblastoma models [22]. Collectively, these considerations position SR9009 and related *NR1D1* agonists not only as monotherapy candidates but also as potentially synergistic partners for chemotherapy and immunotherapy in advanced retinoblastoma.

Several limitations should be acknowledged. First, the number of clinical specimens in our cohort is limited, which constrains broader clinical interpretation. Second, the direct transcriptional targets of *NR1D1* that regulate ROS production remain to be identified. Third, subcutaneous xenografts cannot fully recapitulate the intraocular microenvironment. Future studies using orthotopic models and multi-omics analyses will further clarify the *NR1D1* regulatory network.

In conclusion, our study builds on our previous clinical findings [11] and demonstrates that *NR1D1* is a functional tumor suppressor in retinoblastoma. Low *NR1D1* expression drives RB progression by increasing ROS levels and activating the AKT/mTOR pathway. Pharmacological activation of *NR1D1* by SR9009 significantly inhibits tumor growth in vivo. These findings establish the NR1D1–ROS–AKT/mTOR axis as a critical pathway in RB pathogenesis and identify *NR1D1* as a promising therapeutic target for this childhood malignancy.

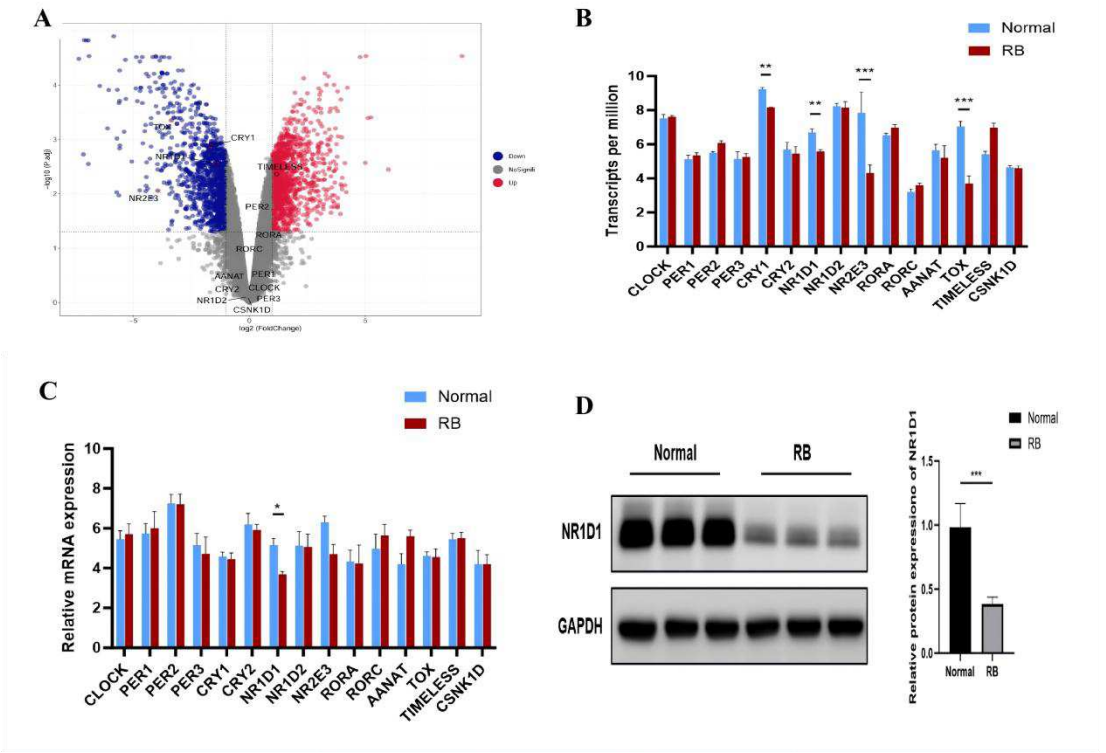


Figure 1. Screening and expression validation of candidate genes in retinoblastoma (RB). (A) Analysis of the GSE58780 dataset from the GEO database was performed to screen differentially expressed genes (DEGs) in RB tissues. A total of 2363 DEGs were identified, consisting of 1207 upregulated and 1156 downregulated genes. (B) Comparison of candidate gene mRNA expression between RB and normal retinal tissues. The mRNA levels of *CRY1* ($P < 0.01$), *NR1D1* ($P < 0.01$), *NR2E3* ($P < 0.001$), and *TOX* ($P < 0.001$) were significantly reduced in RB tissues, whereas *TIMELESS* was significantly upregulated ($P < 0.001$). (C) qPCR analysis demonstrated significant transcriptional downregulation of *NR1D1* at the mRNA level in RB tissues relative to normal retinal tissues. (D) Western blotting confirmed decreased NR1D1 protein expression in RB tissues, consistent with the mRNA expression pattern. Statistical analyses were performed using GraphPad Prism. Two-tailed Student's t-test, Wilcoxon rank-sum test, or one-way ANOVA was used as appropriate; $P < 0.05$ was considered statistically significant.

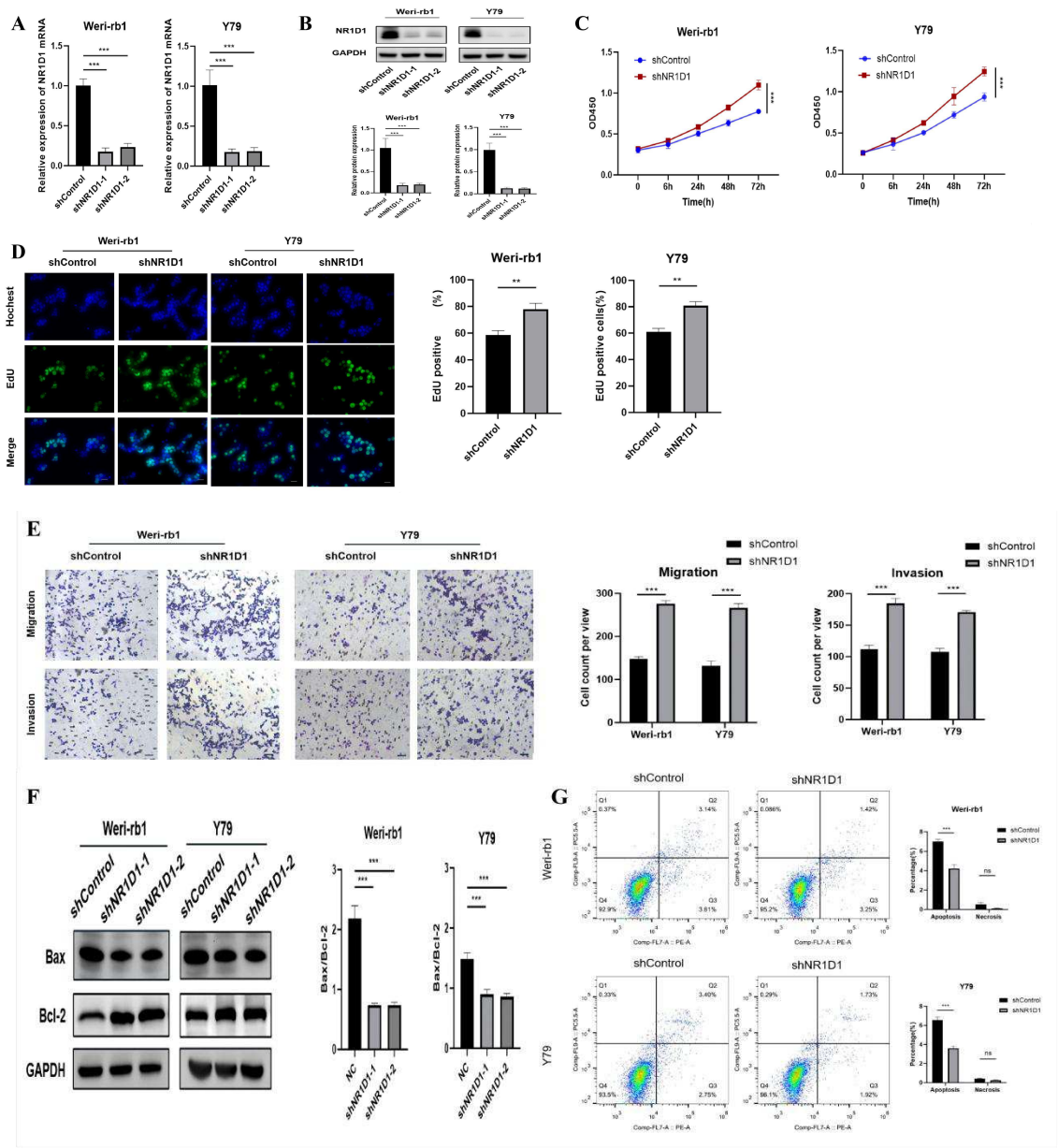


Figure 2. Knockdown of *NR1D1* promotes proliferation, migration, invasion and suppresses apoptosis in retinoblastoma cells. Two shRNA sequences (sh*NR1D1*-1 and sh*NR1D1*-2) were used to silence *NR1D1*. (A) qPCR and (B) western blotting verified the knockdown efficiency at the mRNA and protein levels, respectively. Both shRNAs markedly reduced *NR1D1* mRNA and protein expression compared with the control group. (C) CCK-8 cell viability assays showed that downregulation of *NR1D1* significantly accelerated the proliferation of Weri-Rb1 and Y79 RB cells. (D) EdU assays further demonstrated that the proportion of EdU-positive cells was significantly increased following *NR1D1* knockdown relative to controls. (E) *NR1D1* knockdown enhanced the migration and invasion capacities of RB cells. (F) Western blotting revealed that *NR1D1* knockdown decreased Bax protein expression and increased Bcl-2 protein expression, leading to a reduced Bax/Bcl-2 ratio, indicating suppression of RB cell apoptosis. (G) Flow cytometry confirmed that *NR1D1* silencing significantly attenuated apoptosis in RB cells.

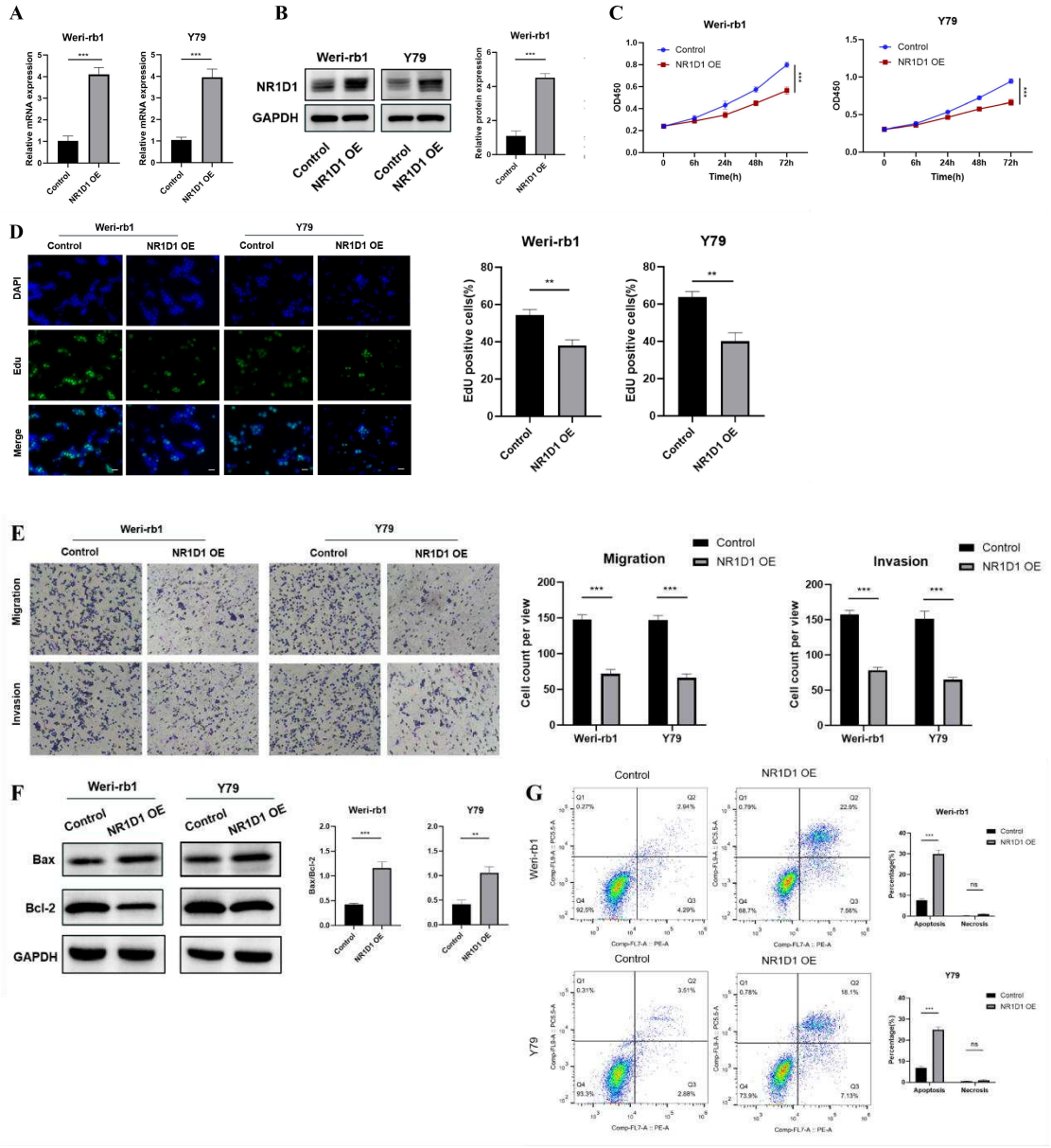


Figure 3. Overexpression of *NR1D1* inhibits malignant phenotypes and promotes apoptosis in retinoblastoma cells. (A, B) qRT-PCR and Western blotting were performed to verify the overexpression efficiency of *NR1D1* in Weri-Rb1 and Y79 RB cell lines. (C) CCK-8 assays indicated that *NR1D1* overexpression significantly suppressed the viability of RB cells. (D) EdU staining showed a reduced proportion of proliferative cells in the *NR1D1*-overexpressing group compared with the control group. (E) Transwell assays demonstrated that ectopic *NR1D1* expression markedly impaired the migration and invasion capacities of RB cells. (F) Western blotting analysis revealed upregulated Bax protein levels, downregulated Bcl-2 protein levels, and an increased Bax/Bcl-2 ratio following *NR1D1* overexpression. (G) Flow cytometry analysis confirmed that enforced *NR1D1* expression significantly induced apoptosis in RB cells.

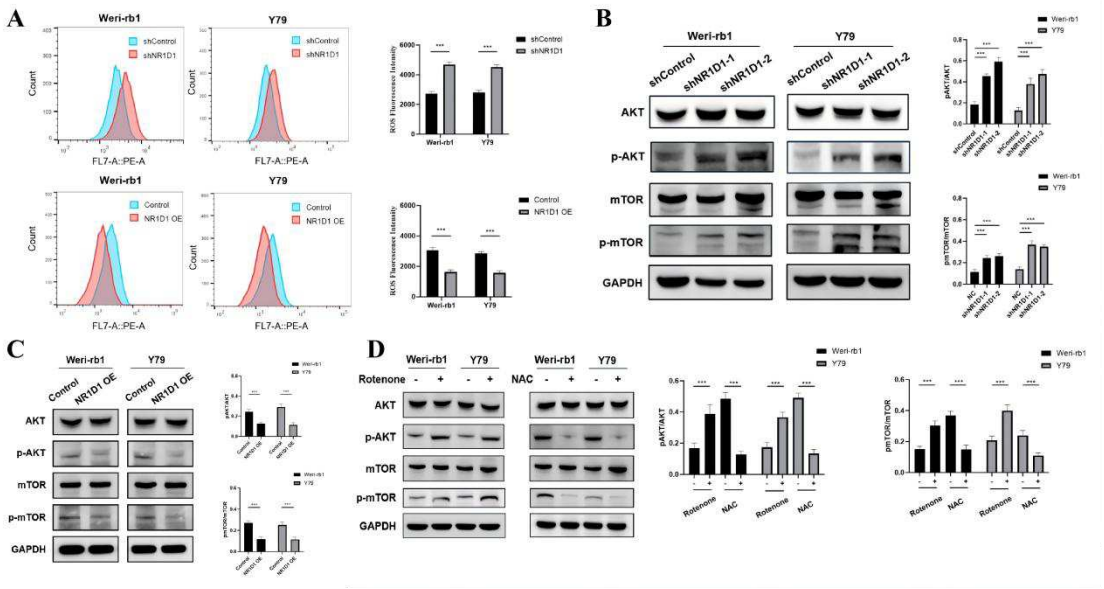


Figure 4. *NR1D1* modulates the AKT/mTOR signaling pathway via regulation of intracellular reactive oxygen species (ROS) in retinoblastoma cells. (A) We investigated the interplay among *NR1D1*, oxidative stress, and AKT/mTOR signaling. *NR1D1* knockdown significantly increased intracellular ROS levels, while *NR1D1* overexpression reduced ROS generation. (B) Western blotting showed that silencing *NR1D1* increased phosphorylation of AKT and mTOR, reflecting pathway activation. (C) Conversely, ectopic *NR1D1* expression suppressed AKT/mTOR signaling. (D) Pharmacological intervention with the ROS inducer rotenone and ROS scavenger N-acetylcysteine (NAC) was performed to validate the causal relationship. Increased ROS activated AKT/mTOR signaling, whereas ROS depletion inhibited AKT/mTOR activity.

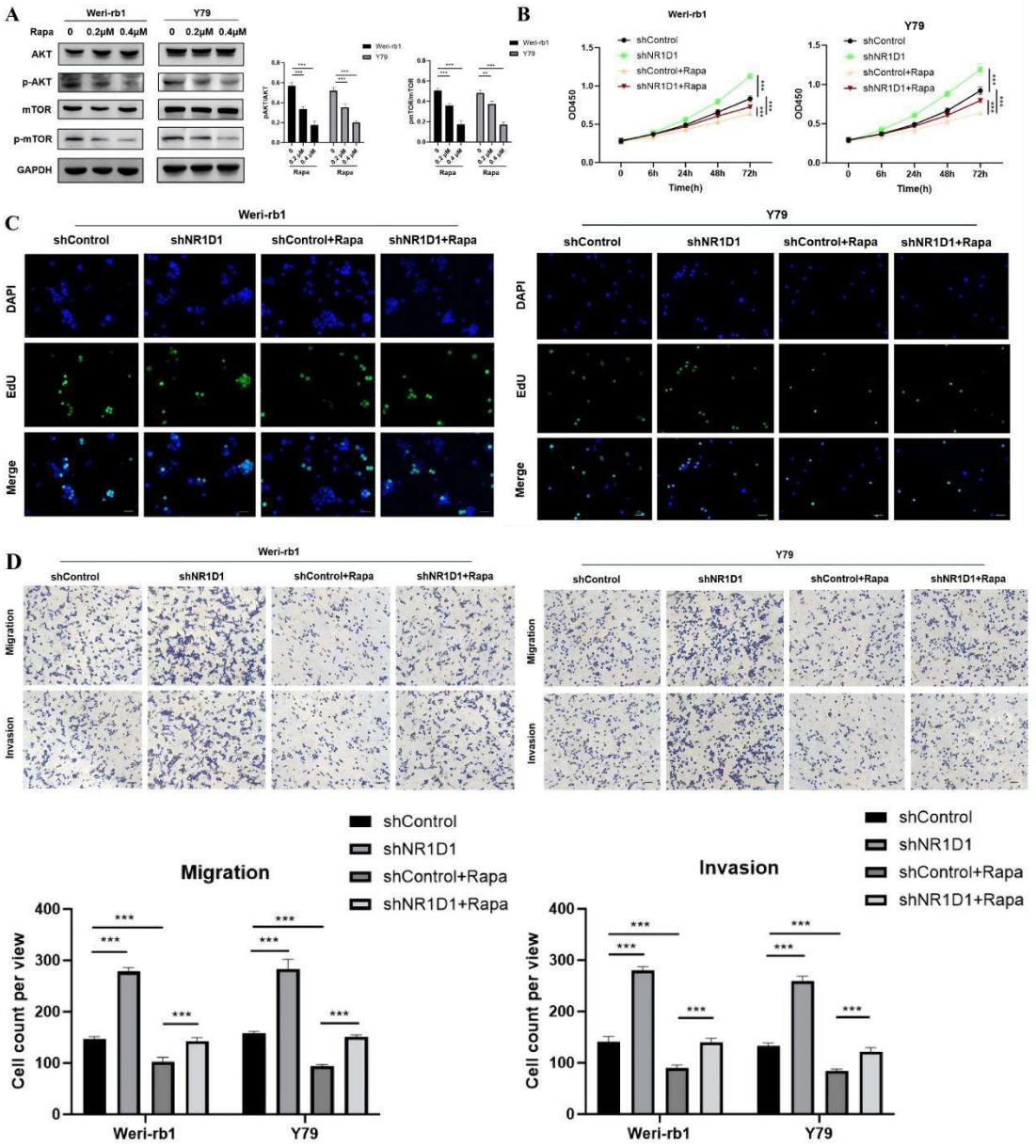


Figure 5. Pharmacological inhibition of mTOR reverses the oncogenic phenotype induced by *NR1D1* knockdown in retinoblastoma cells. (A) RB cells were treated with the mTOR inhibitor rapamycin (Rapa), and rapamycin suppressed AKT/mTOR signaling in a dose-dependent manner. (B, C) Four experimental groups were established: shControl, sh*NR1D1*, shControl + Rapa, and sh*NR1D1* + Rapa. CCK-8 and EdU assays revealed that rapamycin rescued the enhanced cell proliferation triggered by *NR1D1* knockdown. (D) Transwell assays showed that rapamycin also reversed the increased migration and invasion resulting from *NR1D1* silencing. Collectively, these data indicate that the pro-tumor effects of *NR1D1* depletion on RB progression are mediated, at least partially, via the AKT/mTOR signaling pathway.

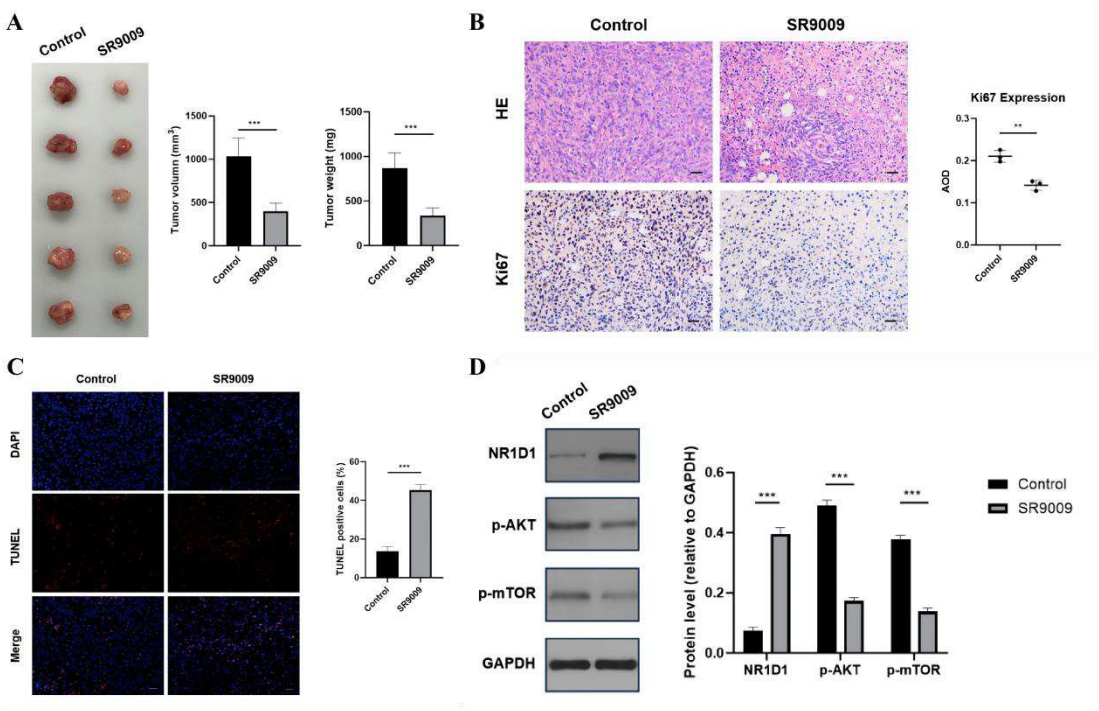


Figure 6. Pharmacological activation of *NR1D1* suppresses retinoblastoma tumor growth and inhibits AKT/mTOR signaling in vivo. (A) A subcutaneous RB xenograft mouse model was established to evaluate the therapeutic potential of *NR1D1* activation. Treatment with the *NR1D1* agonist SR9009 significantly reduced xenograft tumor volume and weight. (B) IHC staining demonstrated decreased Ki-67 positivity in SR9009-treated tumor tissues, indicating suppressed tumor cell proliferation. (C) TUNEL assays revealed a markedly increased proportion of apoptotic cells in the SR9009 treatment group compared with the control group. (D) Western blotting analysis of xenograft tumor tissues showed that SR9009 treatment upregulated NR1D1 protein expression and reduced the phosphorylation levels of AKT and mTOR, confirming the inhibitory effect of SR9009 on the AKT/mTOR signaling pathway in vivo.

Reference:

[1] Global Retinoblastoma Study Group. The Global Retinoblastoma Outcome Study: a prospective, cluster-based analysis of 4064 patients from 149 countries. Lancet Glob Health. 2022 Aug;10(8):e1128-e1140.

[2] Munier FL, Beck-Popovic M, Chantada GL, Cobrinik D, Kivelä TT, Lohmann D, Maeder P, Moll AC, Carcaboso AM, Moulin A, Schaiquevich P, Bergin C, Dyson PJ, Houghton S, Puccinelli F, Vial Y, Gaillard MC, Stathopoulos C. Conservative management of retinoblastoma: Challenging orthodoxy without compromising the state of metastatic grace. "Alive, with good vision and no comorbidity". Prog Retin Eye Res. 2019 Nov;73:100764.

[3] Kaewkhaw R, Rojanaporn D. Retinoblastoma: Etiology, Modeling, and Treatment. Cancers (Basel). 2020 Aug 16;12(8):2304.
[4] Sulli G, Lam MTY, Panda S. Interplay between Circadian Clock and Cancer: New Frontiers for Cancer Treatment. Trends Cancer. 2019 Aug;5(8):475-494.
[5] Sahar NE, Qadir J, Riaz SK, et al. Dysregulated expression of suppressor loop of circadian rhythm genes in colorectal cancer pathogenesis. Minerva Med, 2022, 113(3): 497-505.
[6] Yang Y, Bai Y, Wang X, Guo Y, Yu Z, Feng D, Zhang F, Li D, Han P. Clock gene NR1D1 might be a novel target for the treatment of bladder cancer. Urol Oncol. 2023 Jul;41(7):327.e9-327.e18.
[7] Wang H, Fu Y. NR1D1 suppressed the growth of ovarian cancer by abrogating the JAK/STAT3 signaling pathway. BMC Cancer. 2021 Jul 30;21(1):871.
[8] Shen W, Zhang W, Ye W, Wang H, Zhang Q, Shen J, Hong Q, Li X, Wen G, Wei T, Zhang J. SR9009 induces a REV-ERB dependent anti-small-cell lung cancer effect through inhibition of autophagy. Theranostics. 2020 Mar 15;10(10):4466-4480.
[9] Sun, J., Zheng, Z., Chen, Q., Pan, Y., Lu, H., Zhang, H., Yu, Y., & Dai, Y. (2019). NRF3 suppresses breast cancer cell metastasis and cell proliferation and is a favorable predictor of survival in breast cancer. OncoTargets and therapy, 12, 3019–3030.
[10] Leung YK, Lee SG, Wang J, Guruvaiah P, Rusch NJ, Ho SM, Park C, Kim K. The Loss of an Orphan Nuclear Receptor *NR2E3* Augments Wnt/β-catenin Signaling via Epigenetic Dysregulation that Enhances Sp1-β catenin-p300 Interactions in Hepatocellular Carcinoma. Adv Sci (Weinh). 2024 Aug;11(29):e2308539.
[11] Ding J, Sun J, Ma RQ, Zheng K, Han YN. Low expression of NR1D1 and NR2E3 is associated with advanced features of retinoblastoma. Int Ophthalmol. 2024 Mar 14;44(1):133.
[12] Francis JH, Richards AL, Mandelker DL, Berger MF, Walsh MF, Dunkel IJ, Donoghue MTA, Abramson DH. Molecular Changes in Retinoblastoma beyond RB1: Findings from Next-Generation Sequencing. Cancers. 2021; 13(1):149.
[13] Sulli G, Lam MTY, Panda S. Interplay between Circadian Clock and Cancer: New Frontiers for Cancer Treatment. Trends Cancer. 2019 Aug;5(8):475-494.
[14] El-Hefnawy NE, Youssef MM, Abol-Enein H, Gabal RA. mTOR pathway targeted inhibition via Rapamycin-loaded PLGA nanoparticles for enhanced bladder cancer therapy. Sci Rep. 2025 Jul 2;15(1):23138.
[15] Lv Z, Yang R, Wu J, Shi X, Wang R, Niu Y, Qian Z, Jiao J, Ma Y. NR1D1 in tumorigenesis: dual roles, mechanisms, and therapeutic targeting. Gene. 2026 Jan 20;977:149889.
[16] Mullin NK, Bohrer LR, Voigt AP, Lozano LP, Wright AT, Bonilha VL, Mullins RF, Stone EM, Tucker BA. *NR2E3* loss disrupts photoreceptor cell maturation and fate in human organoid models of retinal development. J Clin Invest. 2024 Apr 23;134(11):e173892.
[17] Welch RD, Billon C, Kameric A, Burris TP, Flaveny CA. REV-ERBα heterozygosity produces a dose-dependent phenotypic advantage in mice. PLoS One. 2020 May 14;15(5):e0227720.

[18]Lastwika KJ, Wilson W 3rd, Li QK, Norris J, Xu H, Ghazarian SR, Kitagawa H, Kawabata S, Taube JM, Yao S, Liu LN, Gills JJ, Dennis PA. Control of PD-L1 Expression by Oncogenic Activation of the AKT-mTOR Pathway in Non-Small Cell Lung Cancer. Cancer Res. 2016 Jan 15;76(2):227-38.
[19] Huang S, Liu CH, Wang Z, Fu Z, Britton WR, Blomfield AK, Kamenecka TM, Dunaief JL, Solt LA, Chen J. REV-ERBα regulates age-related and oxidative stress-induced degeneration in retinal pigment epithelium via NRF2. Redox Biol. 2022;51:102261.
[20] Wang R, Liu SL, Guo QQ, Shi XH, Ma MM. Circadian clock REV-ERBs agonist SR9009 induces synergistic antitumor activity in multiple myeloma by suppressing glucose-regulated protein 78-dependent autophagy and lipogenesis. World J Oncol. 2023;14(6):464-475.
[21] Ka NL, Park MK, Kim SS, Jeon Y, Hwang S, Kim SM, Lim GY, Lee H, Lee MO. NR1D1 stimulates antitumor immune responses in breast cancer by activating cGAS-STING signaling. Cancer Res. 2023;83(18):3045-3058.
[22] Dierickx P, Emmett MJ, Jiang C, Uehara K, Liu M, Adlanmerini M, Lazar MA. SR9009 has REV-ERB-independent effects on cell proliferation and metabolism. Proc Natl Acad Sci U S A. 2019;116(25):12147-12152.